PDR

EGG-TFBP-5900

June 1982

OPERATIONAL TRANSIENT TEST SERIES

TEST OPT 1-2

QUICK LOOK REPORT

NRC Research and/or Technical Assistance Rept

Z. R. Martinson
D. J. Osetek
J. D. White

U.S. Department of Energy
Idaho Operations Office • Idaho National Engineering Laboratory

This is an informal report intended for use as a preliminary or working document

Prepared for the
U.S. Nuclear Regulatory Commission
Under DOE Contract No. DE-AC07-76ID01570
FIN No. A6041

EG&G Idaho

EGG-TFBP-5900
June 1982

OPERATIONAL TRANSIENT TEST SERIES
TEST OPT 1-2
QUICK LOOK REPORT

Z. R. Martinson
D. J. Osetek
J. D. White

Approved: R. W. Hanson for R. K. McCardell
R. K. McCardell, Manager
PBF Experimental Specification
and Analysis Branch

D. W. Croucher for P. E. MacDonald
P. E. MacDonald, Manager
LWR Fuel Research Division

LWR Fuel Research Division
Thermal Fuels Behavior Program
EG&G Idaho, Inc.
Idaho Falls, Idaho 83415

EG&G Idaho, Inc.

FORM EG&G-398
(Rev. 11-79)

INTERIM REPORT

Accession No. _____

Report No. EGG-TFBP-5900

Contract Program or Project Title:

Thermal Fuels Behavior Program

Subject of this Document:

Operational Transient Test Series, OPT 1-2 Test Series Quick Look Report

Type of Document:

Quick Look Report

Author(s): Z. R. Martinson
D. J. Osetek
J. D. White

Date of Document:

June 1982

Responsible NRC Individual and NRC Office or Division:

M. Silberberg

This document was prepared primarily for preliminary or internal use. It has not received full review and approval. Since there may be substantive changes, this document should not be considered final.

EG&G Idaho, Inc.
Idaho Falls, Idaho **83415**

Prepared for the
U.S. Nuclear Regulatory Commission
Washington, D.C.
Under DOE Contract No. **DE-AC07-76ID01570**
NRC FIN No. A6041

INTERIM REPORT

ABSTRACT

The preliminary results of Test OPT 1-2 are discussed in this report. Test OPT 1-2 was performed for the Nuclear Regulatory Commission to address the following two safety issues: (a) should regulations be imposed to limit fuel rod failure during an anticipated transient without scram (ATWS)?, and (b) should reactors be modified to reduce the probability of a severe ATWS occurring? Test OPT 1-2 was performed to evaluate the probability and extent of fuel rod damage for the most severe boiling water reactor ATWS that results in boiling transition, a main steamline isolation valve closure transient without scram. Two sets of two fuel rods in series were tested. An unirradiated fuel rod was used to heat the coolant to typical BWR conditions for a previously irradiated fuel rod. Following an extensive fuel conditioning period of operation, a single power transient was performed that simulated the power history and coolant conditions calculated for a main steam line isolation valve closure ATWS.

A peak test rod power of 300 kW/m, a radially averaged peak fuel enthalpy of 95 cal/g and a peak cladding surface temperature of 1070 K were reached during the 20 minute long transient. The fission product detection system and the loop radiation monitor both indicated that one or more of the fuel rods was leaking after the transient. Since one of the four fuel rods had developed a cladding defect allowing fission product gases to escape prior to the power transient, it was not possible to determine from the on-line data if any of the test rods failed as a result of the power transient. Metallurgical examination will be performed to identify which rod failed prior to the transient and the extent of cladding damage incurred during the transient.

SUMMARY

Anticipated nuclear power transients are deviations from normal plant operating conditions that result from system component malfunctions which may occur one or more times during the service life of a reactor and are normally accompanied by a control rod scram. They are distinguished from "accidents" which have a much lower probability of occurrence. Frequently the effect of the malfunction which initiates the transient results in a loss of the secondary heat sink and a subsequent increase in the system pressure which causes a positive reactivity feedback and an associated power increase. Many of the anticipated transients may be postulated to occur with a failure of the automatic scram system and are then termed "anticipated transients without scram (ATWS)". Departure from nucleate boiling and film boiling are not currently predicted to occur for any pressurized water reactor PWR ATWS event. The potential for fuel rod damage may be higher, however, for BWR ATWS events than for BWR anticipated transients with scram because boiling transition and high cladding temperatures are predicted to occur for the most severe BWR ATWS events. According to vendor safety analyses, the most severe BWR ATWS (the main steamline isolation valve closure transient without scram) would result in a reactor power increase to 745% of rated power for a short period of time followed by low magnitude power oscillations for about 20 minutes before the reactor could be made subcritical by boron injection. Peak cladding temperatures up to ∿1050 K for about 80 s are also calculated to occur. This scenario suggests several fuel rod cladding damage mechanisms: (a) pellet-cladding mechanical, and possibly chemical, interaction; (b) boiling transition and high cladding temperatures causing cladding oxidation and embrittlement; and (c) cladding collapse and waisting (collapse of the cladding into the space between pellets).

At cladding temperatures in excess of the recrystallization temperature (∿920 K), cladding collapse onto the fuel stack and into fuel pellet interfaces has been observed in previous PBF tests, but cladding collapse has not caused failure. At higher temperatures, cladding

oxidation of the outer surface due to zircaloy-water reaction and of the inner surface due to zircaloy-UO_2 reaction becomes appreciable. As oxygen diffuses into the inner and outer cladding surface, the zircaloy undergoes a metallurgical phase transformation from the beta phase to ZrO_2 and the oxygen-stabilized alpha phase. Only the central beta phase retains the integrity and strength of the cladding wall because the ZrO_2 and oxygen-stabilized alpha zircaloy layers are brittle. However, significant zircaloy oxidation would not be expected to occur at the cladding temperatures and durations in boiling transition calculated to occur for even the most severe BWR ATWS.

Since the first indication that zircaloy cladding might be susceptible to failure caused by a pellet-cladding interactive mechanism, the phenomena has received considerable attention. PCI failures during slow power increases are apparently induced after sufficiently high burnup is attained to allow fission product release. PCI cladding cracking is usually prevented during normal operation by using very slow rates of reactor power increase. Pellet-cladding mechanical interaction failures may also occur during very fast power increases such as occurs during a severe BWR ATWS due to high strain rate tearing or fracture of irradiation embrittled zircaloy cladding. Since the most severe anticipated transients without scram have not actually occurred and applicable data is not available, the Nuclear Regulatory Commission was uncertain whether light water reactor (LWR) irradiated fuel rods would fail or even be damaged as a result of these transients. Therefore the Nuclear Regulatory Commission requested that simulated ATWS testing be performed to address the following two safety issues: (a) should regulations be imposed to limit fuel rod failure during an ATWS?, and (b) should reactors be modified to reduce the probability of a severe ATWS occurring? Accordingly, Test OPT 1-2 was conducted on May 24, 1982 in the Power Burst Facility (PBF) at the Idaho National Engineering Laboratory by EG&G Idaho, Inc.

Test OPT 1-2 was performed to evaluate the probabilty and extent of fuel rod damage for the most severe BWR ATWS that results in boiling transition. The test consisted of two sets of two fuel rods in series.

The purpose of the first unirradiated rod in each set was to provide coolant conditions for the second irradiated test fuel rod which were typical of the coolant conditions existing near the axial flux peak region of a commercial BWR core. Following an extensive fuel conditioning operation, a single power transient was performed that simulated a main steam line isolation valve closure ATWS at near-typical BWR coolant pressure, quality, and flow rate conditions calculated to exist during such an ATWS.

A peak test rod power of 300 kW/m, a radially averaged peak fuel enthalpy of 95 cal/g UO_2, and a maximum measured cladding surface temperature of ~1070 K were reached during the 20 minute transient. The fission product detection system and the loop radiation monitor both indicated that one or more of the four fuel rods was leaking after the transient. Since a leak had developed in either one of the two heater rods or one of the irradiated test rods during the fuel conditioning operation prior to the power transient it was not possible to determine from the on-line data if either of the test rods failed as a result of the transient. Post-test metallurgical examination will be performed to determine which rod failed prior to the transient and the extent of test rod cladding damage caused by the transient.

CONTENTS

FIGURES

TABLES

1. INTRODUCTION

Anticipated nuclear power reactor transients are deviations from normal plant operating conditions that result from system component malfunctions which may occur one or more times during the service life of a reactor and are normally accompanied by a control rod scram. They are distinguished from "accidents" which have a much lower probability of occurrence. Frequently the effect of the malfunction which initiates the transient results in a loss of secondary heat sink and a subsequent increase in system pressure which causes a positive reactivity feedback and associated power increase.

Many of the operational transients may be postulated to occur with a failure of the automatic scram system and are then termed anticipated transients without scram (ATWS). The probability of failure of a light water reactor scram system per demand is in dispute, but the likely range is from 10^{-4} to 10^{-6}. The range of probabilities for the occurrence of an ATWS based on an anticipated transient with a probability of occurrence of once per reactor year is therefore 10^{-4} to 10^{-6} per reactor year. ATWS events were elevated in status with the publication of NUREG-0460, Vols. I and II in 1978.[1] This report reviewed available information on the subject and incorporated analyses performed by the vendors. A later volume of the report suggested that resolution of the ATWS concern should rest on engineering evaluation and judgement of the appropriateness of alternative plant modifications, rather than quantitative risk analyses. In pressurized water reactors (PWR) the reactivity feedback due to collapse of steam voids is small compared to BWR's. Therefore, the power increases calculated to occur in PWR anticipated transients with and without scram are much less than in BWR's. Departure from nucleate boiling (DNB) is not currently predicted to occur for any PWR ATWS event.

The potential for fuel rod damage may be higher for BWR ATWS events than for BWR anticipated transients with scram. The most severe BWR ATWS, according to vendor safety analyses[2] would result in reactor power increases up to 745% of the rated power for a short period of time followed by low magnitude power oscillations for 20 minutes before the reactor is

made subcritical by boron injection. Peak cladding temperatures up to ≈1050 K for about 80 s are also predicted. This scenario suggests several fuel rod damage mechanisms: (a) pellet cladding mechanical interaction (PCI), (b) boiling transition causing cladding oxidation and embrittlement; and (c) cladding collapse and waisting, (collapse of the cladding into the space between pellets).

At cladding temperatures in excess of the recrystallization temperature (∿920 K), cladding collapse onto the fuel stack and into fuel pellet interfaces has been observed in previous PBF tests, but cladding collapse has not caused failure. At higher temperatures, cladding oxidation of the outer surface due to zircaloy-water reaction and of the inner surface due to zircaloy-UO_2 reaction becomes appreciable. As oxygen diffuses into the inner and outer cladding surface, the zircaloy undergoes a metallurgical phase transformation from the beta phase to ZrO_2 and oxygen-stabilized alpha phase. Only the central beta phase retains the integrity and strength of the cladding wall due to the brittle nature of the ZrO_2 and oxygen-stabilized alpha zircaloy layers. Significant zircaloy oxidation would not be expected to occur at the cladding temperatures and durations in boiling transition calculated to occur for even the most severe BWR ATWS.

The first indication that zircaloy-clad UO_2 fuel rods might be susceptible to failure due to a pellet-cladding interaction (PCI) mechanism inherent to the fuel and cladding materials was obtained in 1964 by General Electric in the "High Performance UO_2 Program" jointly sponsored by the United States Atomic Energy Commission and EURATOM.[3] Since that time the phenomena of pellet-cladding interaction induced cladding failure has received considerable attention throughout the world. PCI failures during slow power increases are apparently induced after sufficiently high burnup is attained to allow fission product release. Experiments involving near normal operation power ramp rates have been performed in the Halden, Studsvik, NRU, GETR, RISO RCN-Petten, BR-2 and BR-3 reactors.[4-9] Most investigators now accept the view that both the presence of aggressive chemical species and high localized stresses are prerequisites for normal operation, power ramp induced pellet-cladding interaction failures.

However, pellet-cladding mechanical interaction failures may also occur during very fast power increases due to high strain rate tearing or overstress fracture of irradiation embrittled zircaloy cladding.[10] Results from experimental programs completed or underway to determine the power, ramp rate, and burnup dependency of PCI failures during relatively slow power ramps indicate that incipient cladding cracks may occur in some fuel designs at power levels within commercial reactor operating ranges. Such cladding cracking is usually prevented during normal operation by using very slow rates of reactor power increase. However, certain ATWS events cause a rapid change in power.

Since an ATWS has never actually occurred and applicable data is not available, the Nuclear Regulatory Commission was uncertain whether light water reactor (LWR) irradiated fuel rods would fail or even be damaged as a result of these transients. Therefore, the Nuclear Regulatory Commission (NRC) requested that ATWS testing be performed to address the following two safety issues: (a) should regulations be imposed to limit fuel rod failure during an ATWS? and (b) should reactors be modified to reduce the probability of a severe ATWS occurring? Accordingly, Test OPT 1-2 was conducted in the Power Burst Facility (PBF) at the Idaho National Engineering Laboratory by EG&G Idaho, Inc.

Test OPT 1-2 was performed to evaluate the probability and extent of fuel rod damage for the most severe BWR ATWS that results in boiling transition. Two sets of two fuel rods in series were tested. The purpose of the first unirradiated rod in each set was to provide coolant conditions for the second irradiated test fuel rod which were typical of the coolant conditions existing near the axial flux peak region of a commercial BWR core. Following an extensive fuel conditioning operation, a single power was performed that simulated a main steam isolation valve closure transient without scram at near-typical coolant pressure, quality, and flow rate conditions that are calculated to exist during such an ATWS.

Test OPT 1-2 was conducted with two previously irradiated[a] BWR 8 x 8 fuel rods fabricated by the General Electric Company and two unirradiated 8 x 8 fuel rods fabricated by EG&G Idaho, Inc. The two irradiated fuel rods were of typical GE 8 x 8 design, except for fuel length (0.75 m). The two unirradiated heater fuel rods were enriched to 10 wt% ^{235}U to provide sufficient power to produce the required coolant conditions.

Each fuel rod was surrounded by a coolant flow shroud. The outlets of the heater rod flow shrouds were connected by tubing to the inlets of the irradiated test rod flow shrouds. A schematic of a pair of fuel rods and the coolant flow path is shown in Figure 1. Remotely operated orifices, installed at the heater rod shroud outlets provided a means of reducing the coolant flow for the test rods by about 55% prior to the power transient. The variable orifice design was necessary to obtain the required low flow rates for the test fuel rods without causing severe failure of the much higher power heater rods prior to the transient. A cross section of the fuel rods, flow shrouds and the test train is shown in Figure 2. The two irradiated test rods were each instrumented with three thermocouples (0.7 mm diameter, zircaloy sheathed, tungsten-rhenium) resistance welded to the outer cladding surface. A linear variable differential transformer (LVDT) measured the axial elongation of each fuel rod. Additional instrumentation was provided to measure coolant conditions, fuel rod power, and fission product release characteristics.

The overall experiment requirements and objectives for the OPTRAN Test Series are described in the Experiment Requirements Document,[11] while the experiment specifications for Test OPT 1-2 are described in References 12 and 13, pretest predictions are described in Reference 14, and experiment operating specifications are described in Reference 15.

---

a. The two GE fuel rods were irradiated in the Monticello BWR which is owned and operated by Northern States Power Company.

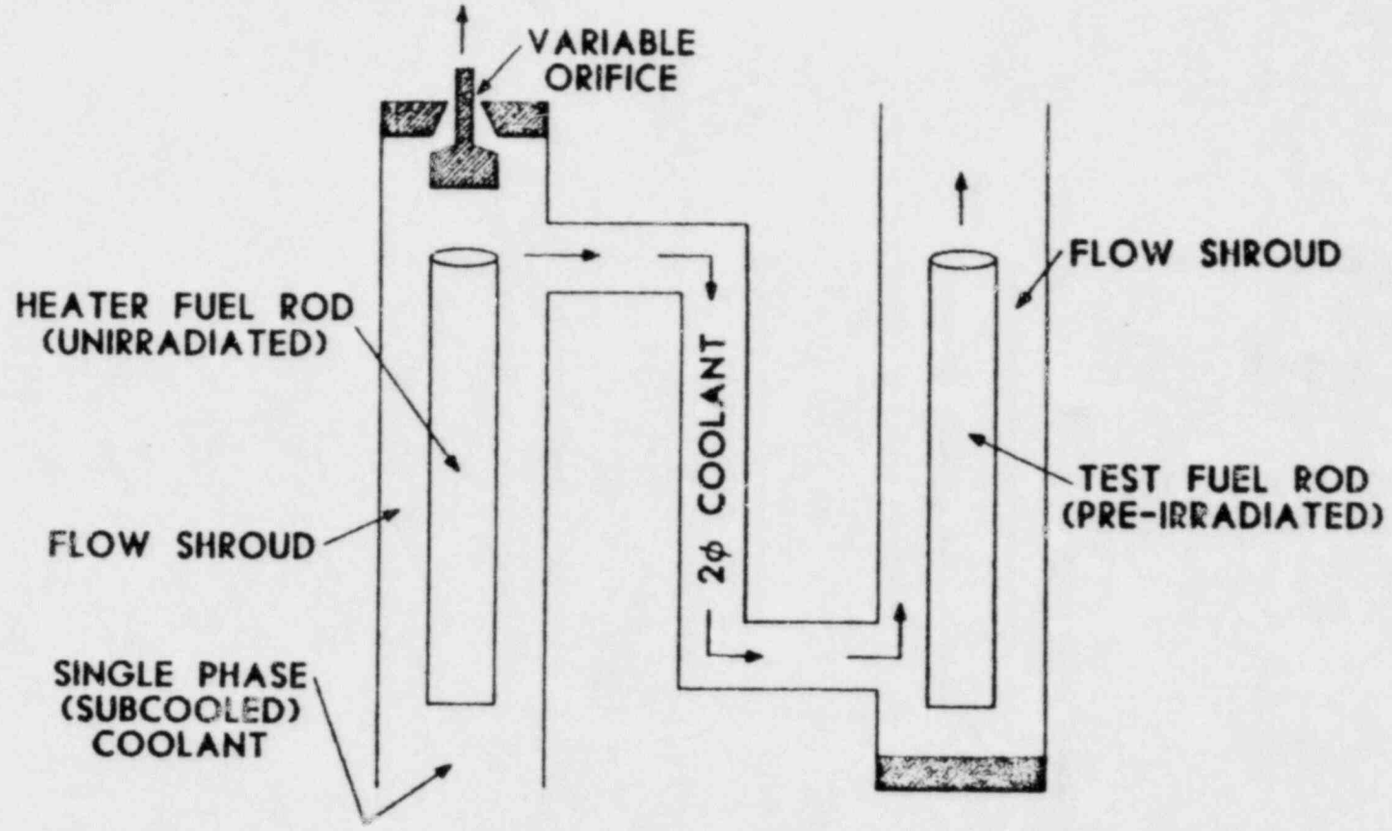

Figure 1. Schematic of fuel rod shroud pair showing flow path.

Fuel rod/shroud assembly positions

quadrant 1 - rod 902-1
quadrant 2 - rod 902-2
quadrant 3 - rod 902-3
quadrant 4 - rod 902-4

REACTOR NORTH

The 0-degree position for each flow shroud or fuel rod is toward the center of the assembly.

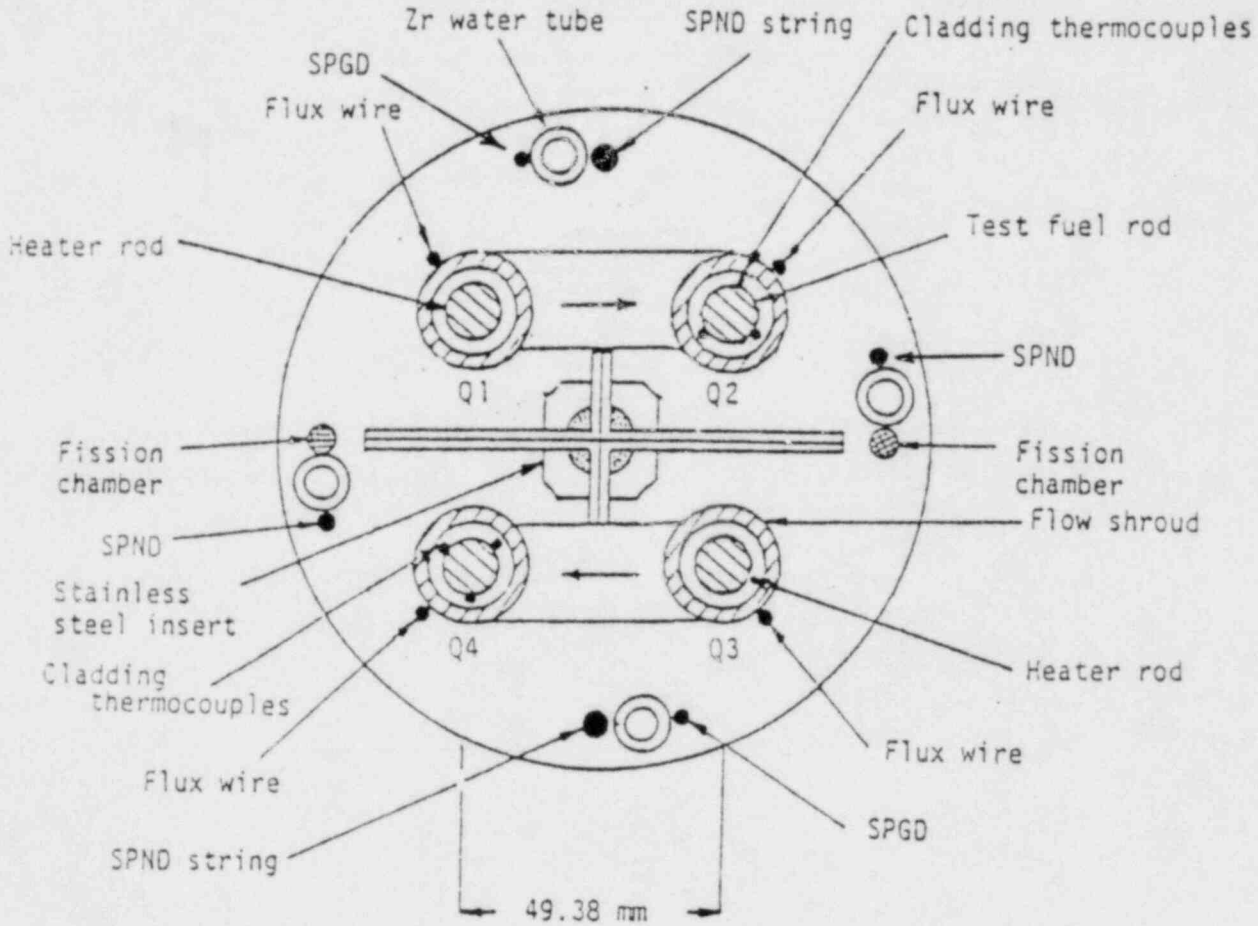

Figure 2. Cross-sectional view of test assembly showing relationship between fuel rods, shrouds, and rod and shroud instrumentation.

The preliminary results of the OPT 1-2 Test Series are discussed in this report. The test conduct is described in Section 2 and the individual fuel rod responses are presented in Section 3. Conclusions based on the OPT 1-2 Test Series results are provided in Section 4. Further details of the test design and test instrumentation are provided in Appendix A.

2. TEST CONDUCT

The nuclear operation for Test OPT 1-2 consisted of an extensive fuel rod conditioning phase and a single power transient. A ∿1 hour power ramp and a ∿3 hour hold at steady reactor power preceded the transient. The non-nuclear operation consisted of two loop heatups and a radionuclide tracer injection in the loop to characterize fission product transport behavior. The test operation is shown schematically in Figure 3. The following subsections describe the test conduct in more detail.

2.1 Heatup Phase

System conditions and experimental measurements were monitored to evaluate instrument performance during the heatup phase. The loop pump was turned off for a few minutes to normalize the coolant pressure transducers to the loop pressure indicated by the Heise gauge. The coolant volumetric flow rate that bypasses the fuel rod shrouds was measured by closing the inpile tube bypass line valves so that all of the loop flow entered the inpile tube. A flow bypass ratio (bypass flow/total heater rod shroud flow) varying from ∿14.4 to 1 at low flow rates (0.3 l/s) to 5.25 to 1 at high flow rates (0.95 l/s) was measured. The maximum loop temperature achievable with the loop electrical heaters was ∿490 K due to heat losses in the loop piping. Nuclear heating during the fuel conditioning phase of the test was required to reach the specified loop temperature of 550 K.

2.2 Samarium Sample Injection

A nine curie sample of ^{153}Sm was injected into the PBF loop prior to final preconditioning of the OPT 1-2 test rods. The objective of the injection was to measure the mixing characteristics of the PBF loop for use in assessing fission product release data. The fission product detection system (FPDS) was used to monitor the samarium during injection and for several hours following injection. Preliminary data accumulated from a single ^{153}Sm photopeak channel are illustrated in Figure 4.

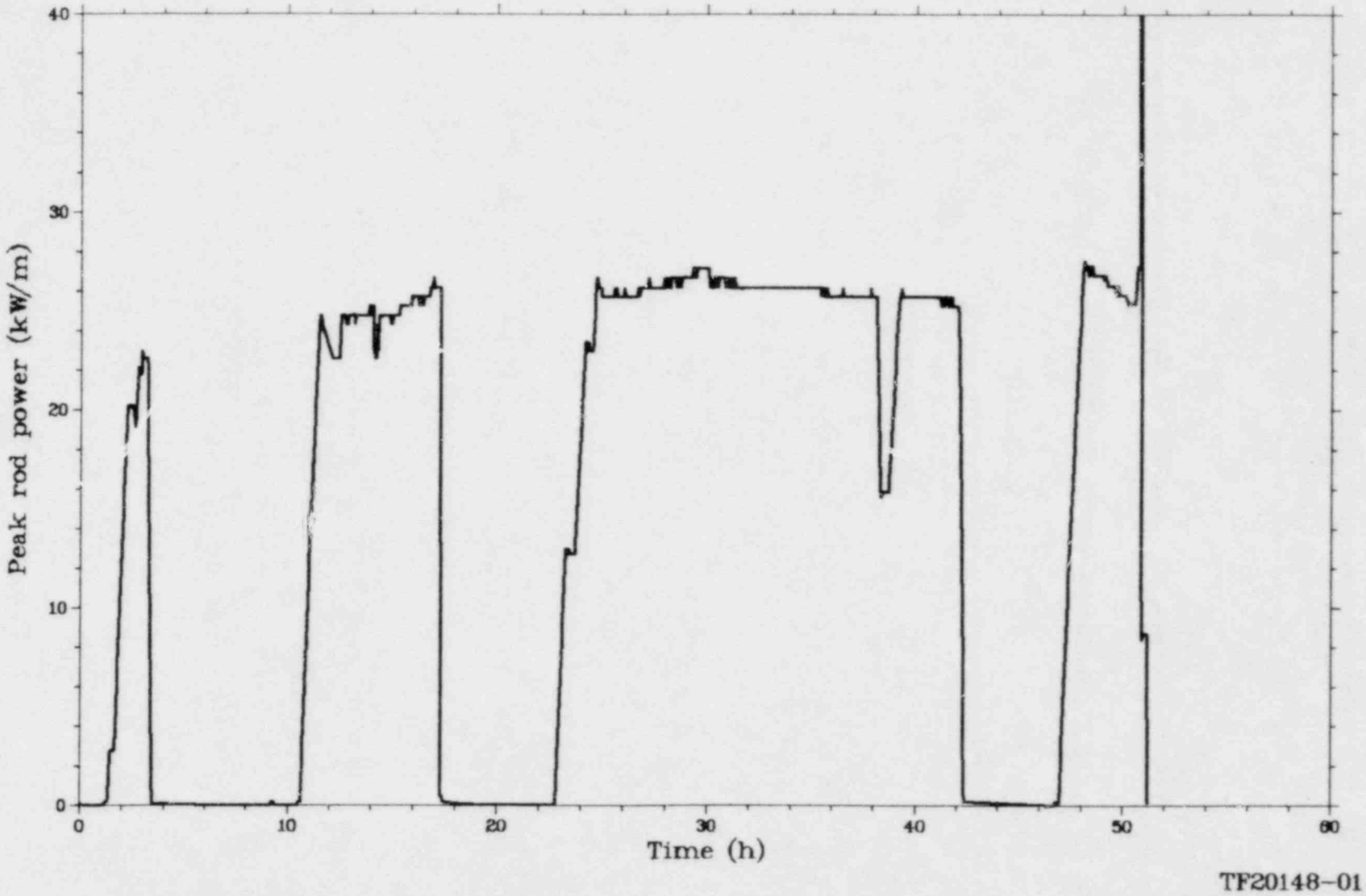

Figure 3. Fuel rod power history during Test OPT 1-2.

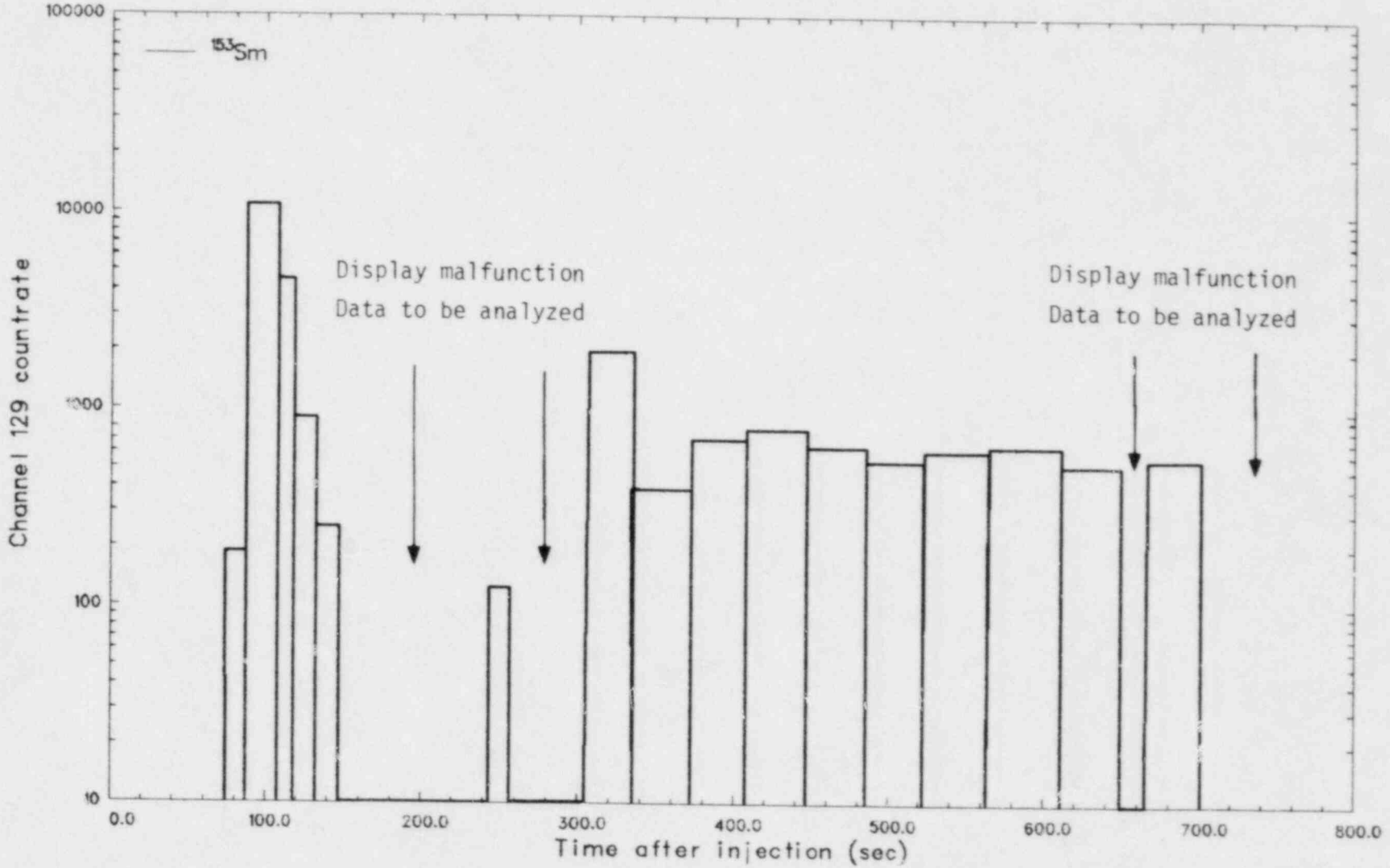

Figure 4. ^{153}Sm concentration behavior in PBF loop coolant following injection.

Within 80 s after initiation of the injection, ^{153}Sm appeared at the FPDS. The measured activity peaked during the next spectrum accumulated and rapidly diminished in the following spectra. A second peak of activity, 1/5 the magnitude of the first, was measured at ∿300 s. The samarium concentration in the loop rapidly attained equilibrium. The photopeak count rate (proportional to concentration) fluctuated less than ±12% from 450 to 700 s. This very short time required to attain concentration equilibrium of a spike release will be useful for reducing the uncertainty in the estimated release rates of fission products during previous PBF tests. The release fraction of an isotope during fuel damage tests in PBF would be expected to quickly (∿7 min) reach a constant value if release from the fuel was short lived. If the release fraction histories (corrected for parent behavior) show a long time (∿15 min) to reach equilibrium, the release from damaged fuel would have to persist for several minutes.

Prior to the sample injection experiment the duration of fission product releases could not be accurately determined, because recirculation and equilibrium mixing times were not known, and long duration releases could not be distinguished from recirculating releases. With the smaller uncertainty on the duration of release, the magnitude of the isotopic release rates can now be more accurately determined. A means to quantitatively assess the durations of fission product releases during previous tests will be developed during the detailed investigation of the ^{153}Sm injection data.

2.3 Fuel Conditioning

The purpose of this test phase was to measure rod powers and to carefully condition the irradiated fuel rods to a peak rod power of ∿29 kW/m since the test rods had been irradiated in the Monticello BWR at a power of only ∿13 kW/m at the edge of the BWR core and a sudden increase in power above 13 kW/m was apt to cause PCI cracking of the cladding. Maximum test rod power ramp rates were held to 0.5 kW/m per minute up to 26 kW/m and 0.35 kW/m per hour for rod powers in excess of 26 kW/m. The fuel conditioning phase was performed with single-phase coolant conditions to measure the rod power.

Three separate periods of nuclear operation as shown in Figure 3 were required to complete the fuel conditioning. The first nuclear operation consisted of a slow power ramp to a test rod peak power of ∿23 kW/m. The reactor was shut down to correct calibration constants for the differential thermocouples and a small leak in the inpile tube head braze plugs. The second nuclear operation consisted of a slow power ramp to a test rod peak power of 27 kW/m. A loop pump trip and reactor scram occurred during the second power ramp at a rod power of 27 kW/m.

The third nuclear operation consisted of a 2 hour power ramp to 27 kW/m and a 5 hour power ramp to 28.5 kW/m. The rod power was then held constant at ∿28.5 kW/m (26.5 MW core power) for the next eight hours. About five hours into the power hold, the plant radiation monitor indicated a factor of ten increase in the radiation level near the loop pressurizer. The reactor power was decreased from 26.5 to 15 MW for ∿1500 s to determine if the indicated radiation level would decrease with reactor power. The radiation level remained the same after the reactor power was decreased and then increased back to 26.5 MW. The reactor power was then held constant at 26.5 MW for the next three hours to complete the planned twelve hour power hold. The test rod peak power had decreased to about 26 kW/m at the end of the 12 hour fuel conditioning due to decreased figure-of-merit (ratio of test rod power to reactor power) caused by control rod withdrawal to compensate for xenon poisoning. Detailed fission product spectum measurements performed the following day confirmed that one of the fuel rods had developed a leak about the time the plant radiation monitor detected an increased radiation level near the pressurizer. It is not known at this time whether one of the previously irradiated test rods or one of the fresh heater rods developed a leak. It was noted that the elongation sensor on previously irradiated test Rod 902-2 decreased about 2 mm during the same time span the radiation monitor increased. A plot of the radiation level and the Rod 902-2 elongation is shown in Figure 5. Reactor power is constant at 26.5 MW during the entire time. Failure of irradiated test Rod 902-2 is suspected but detailed examination will be required to determine which rod was leaking prior to the power transient.

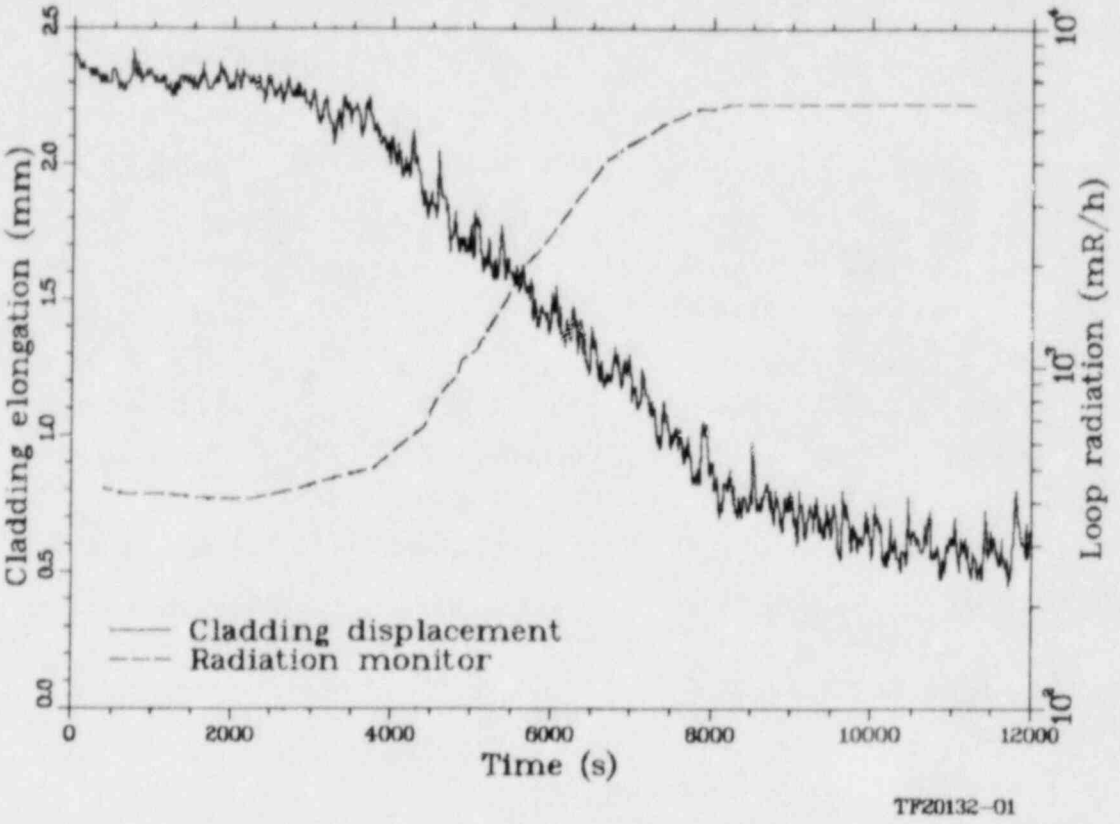

Figure 5. Cladding elongation for test Rod 902-2 and loop radiation vs. time during fuel conditioning of Test OPT 1-2.

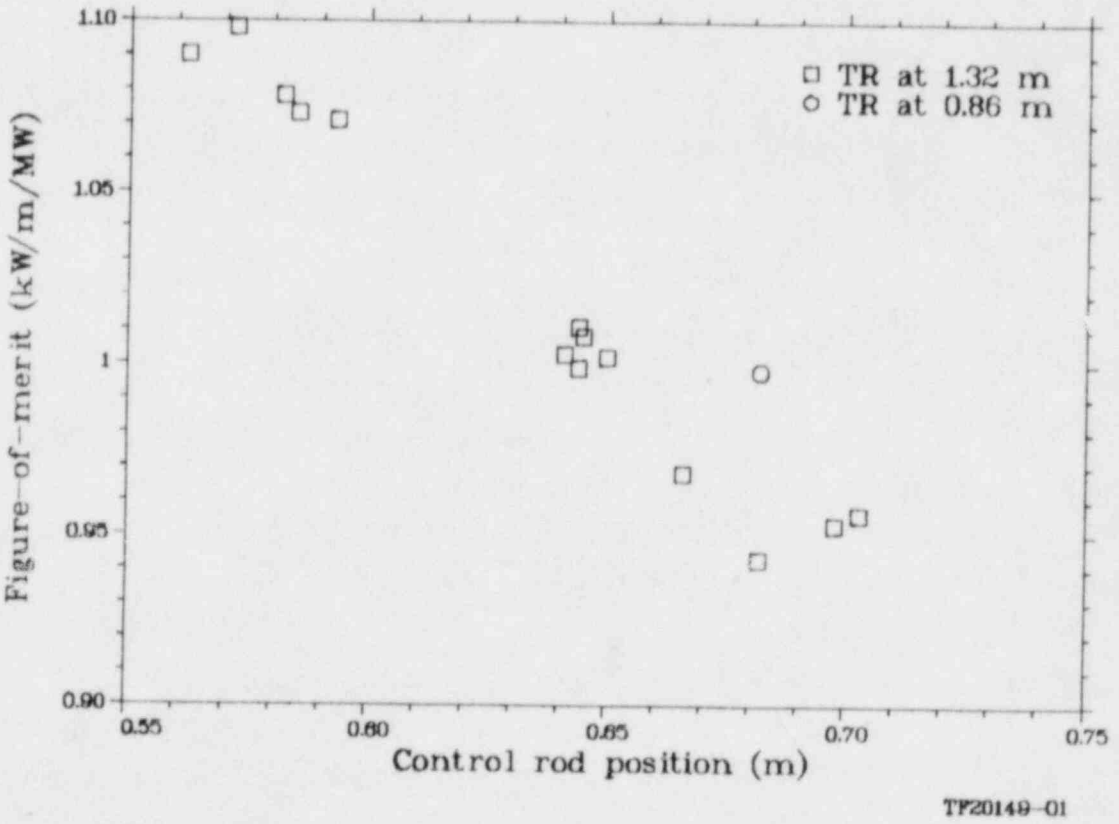

Figure 6. Figure-of-merit (test rod peak power/reactor power) vs. control rod position for Test OPT 1-2.

A plot of the measured figure-of-merit for the test rods as a function of control rod position is shown in Figure 6. The figure-of-merit decreases as the control rods are withdrawn from the core due to a reduction in the core radial power peaking (radial leakage of the neutrons). The transient rods (TR) were positioned at 0.86 m during the power transient to provide sufficient reactivity to perform the power transient (1.32 m full out position). The figure-of-merit decreased about 8% when the transient rods were inserted into the core and the control rods were withdrawn to maintain a constant indicated reactor power. The decrease in figure-of-merit upon transient rod insertion is due to the decreased relative power peaking at the inpile tube when the transient rods are inserted into the core and the control rods are withdrawn.

The average figure-of-merit for the heater rods was about 2.5 times as large as the average figure-of-merit for the test rod (2.49 as compared with 0.96 kW/m per MW, respectively).

2.4 Power Transient

The power transient simulated a BWR main steam isolation valve closure ATWS for irradiated fuel rods operating slightly above BWR core average rod powers. Prior to the power transient, the test rod peak powers were increased to 27 kW/m during a 1-1/2 hr ramp and held constant for about 2 hours. The test rod shroud outlet coolant conditions were initially maintained below saturation temperature to obtain a thermal-hydraulic power calibration of the heater rod and test rod powers.

Saturated water conditions at the inlet of the test rods were then obtained by decreasing the coolant flow rate while keeping the variable orifices closed. Heater rod inlet coolant conditions were 550 K inlet temperature, 300 cm^3s shroud flow rate, and 7.93 MPa coolant pressure. Prior to the power transient, the variable orifices were fully opened to reduce the test rod inlet coolant flows by about 55%.

During an actual BWR main steam isolation valve closure ATWS the recirculation pumps would trip off and the core inlet flow rate would decrease by ~60% over a ~16 s time span. The flow was reduced prior to

the PBF transient to better maintain coolant conditions during the transient since the heater rod flow increased when the orifices were opened, and also to simplify timing the opening of the orifices with respect to the power transient. General Electric analyses for a main steam isolation valve closure ATWS indicate that the coolant pressure will rapidly increase from 7.24 MPa to a peak of about 8.96 MPa and then decrease to about 7.24 MPa over a 20 s time span. Since the PBF loop is not capable of simulating such a rapid pressure surge, a fixed pressure of 7.93 MPa was used for performing the test in PBF. This pressure was chosen because it is near the time-weighted average coolant pressure calculated by GE during the transient. In addition, the 7.93 MPa is equal to the midrange pressure set points of 7.79 to 8.07 MPa for opening the safety/relief valves of a BWR. The recirculation pump trip set point is also 7.93 MPa.

The PBF programmable reactor control system was used to obtain the power transient shown in Figure 7. The transient fuel rod power history was based on General Electric analysis for a fuel rod operating at maximum power. During the transient the peak test rod power increased from 27 to 309 kW/m, at a maximum ramp rate of 300 kW/m per s. The rod power then decreased to 10 kW/m in about 32 s and was then held constant at 10 kW/m for the next ~1170 s. The loop radiation monitor indicated that one or more of the fuel rods was leaking after the transient. The fission product detection system also indicated the presence of a leaking rod(s). Since one of the rods had developed a leak during the fuel conditioning operation prior to the transient, it was not possible to determine from the on-line data if the test fuel rods failed as a result of the transient. Detailed metallurgical examination will be required to identify which rod(s) were leaking.

3. TEST RESULTS

The preliminary results of the LOFT 1-2 power transient are discussed in this section. The on-line data are also compared with pretest FRAP-T6[16] calculations.[a] The FRAPCON-2[17] code[b] was used to calculate the characteristics of the test rods after irradiation in the Monticello BWR. The output of FRAPCON-2 was manually input into FRAP-T6.

3.1 Test Rod Power and Enthalpy

As shown in Figure 7, the peak test rod power increased from 27 to 300 kW/m in about 1.5 s at a maximum ramp rate of 300 kW/m per second. The transient test rod power has been reduced by 3% since the test rod energy per fission was about 3% lower on the average during the transient than the test rod energy per fission during steady-state operation. Based on FRAP-T6 calculations, the radially averaged peak fuel enthalpy increased from 48 to 95 cal/g UO_2 at 2.4 s after the time of peak power. The maximum calculated fuel centerline temperature increased from 1360 to ~2100 K during the transient.

3.2 Test Rod Cladding Surface Temperature

Comparisons of the measured and calculated cladding surface temperatures at 270 mm[c] on Rod 902-2 and at 70 mm[c] on Rods 902-2 and 902-4 are shown with the test rod power in Figures 8, 9, and 10, respectively. The two thermocouples at 170 mm on Rods 902-2 and 902-4 and the thermocouple at 270 mm on Rod 902-4 did not indicate boiling transition occurrence. The thermocouple at 270 mm on Rod 902-2 (Figure 8) indicated a

---

a. FRAP-T6, Idaho National Engineering Laboratory Code Configuration Control Number F00404.

b. FRAPCON-2, Idaho National Engineering Laboratory Code Configuration Control Number H0198828.

c. Thermocouple locations are relative to the axial midplane of the test rod fuel stack (376 mm).

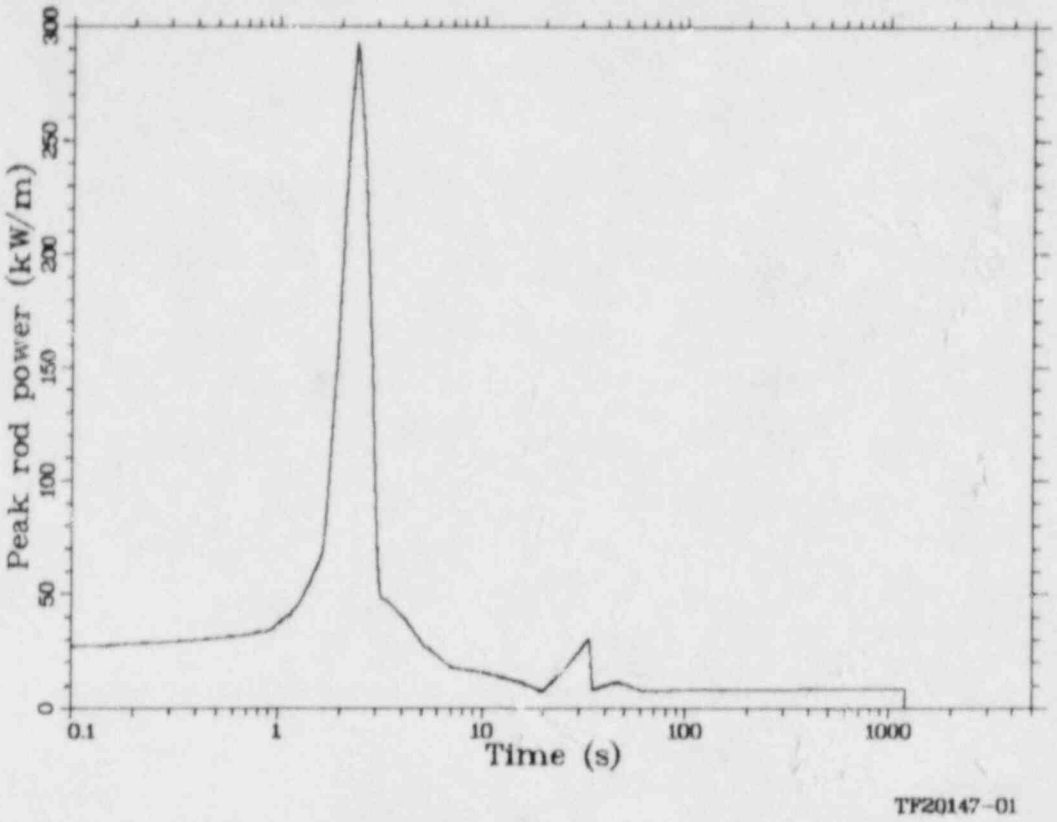

Figure 7. Test rod peak power vs. time during Test OPT 1-2 transient.

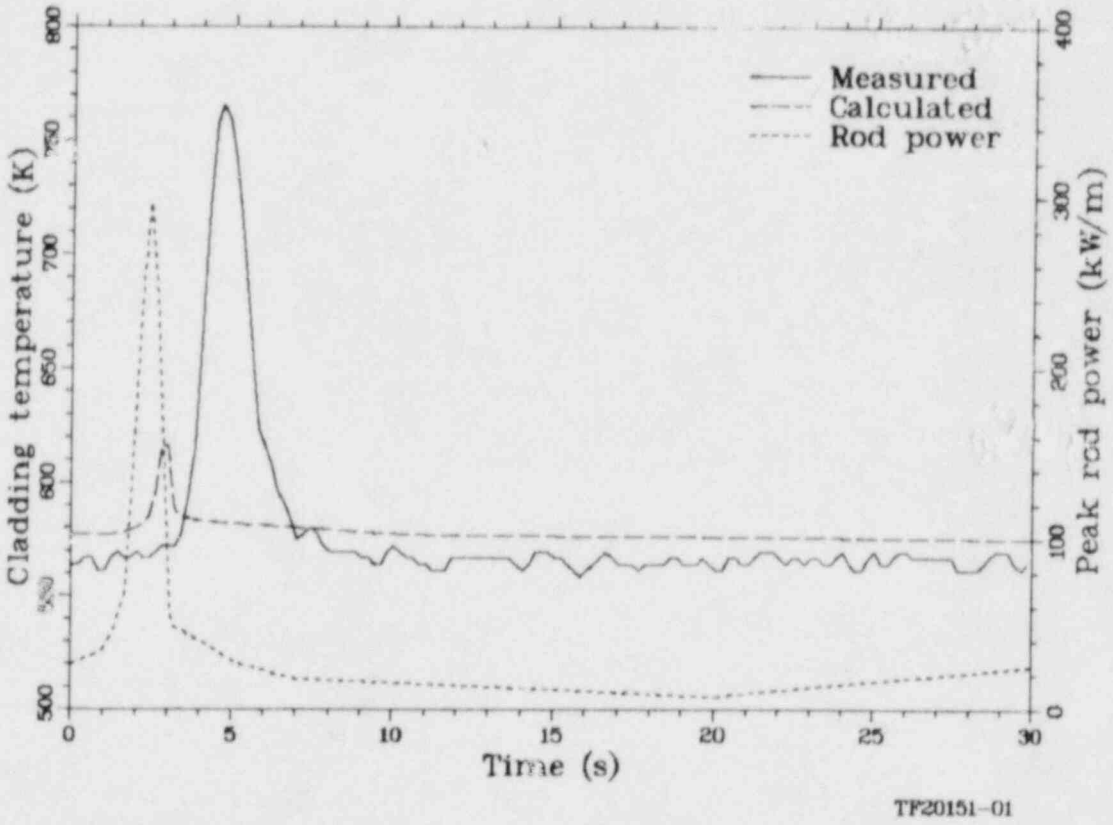

Figure 8. Measured and calculated cladding temperature at 270 mm - 240° thermocouple location and peak rod power vs. time for test Rod 902-2 during Test OPT 1-2 transient.

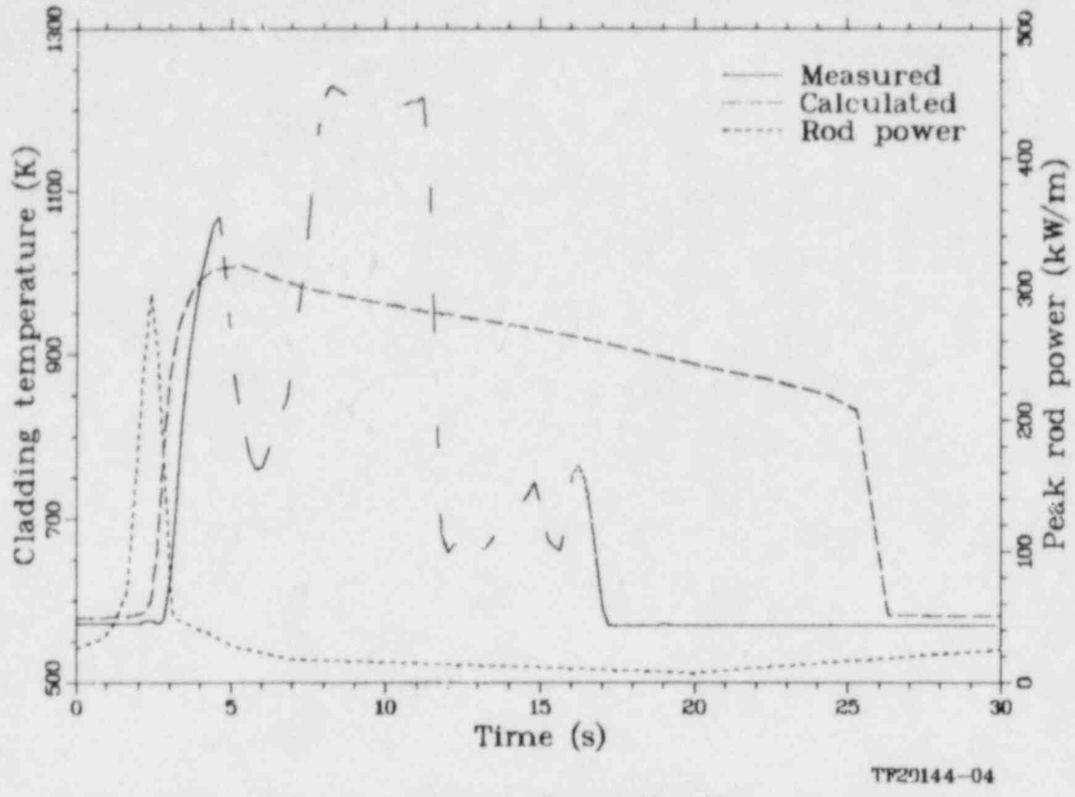

Figure 9. Measured and calculated cladding temperature at 70 mm - 0° thermocouple location and peak rod power vs. time for test Rod 902-2 during Test OPT 1-2 transient.

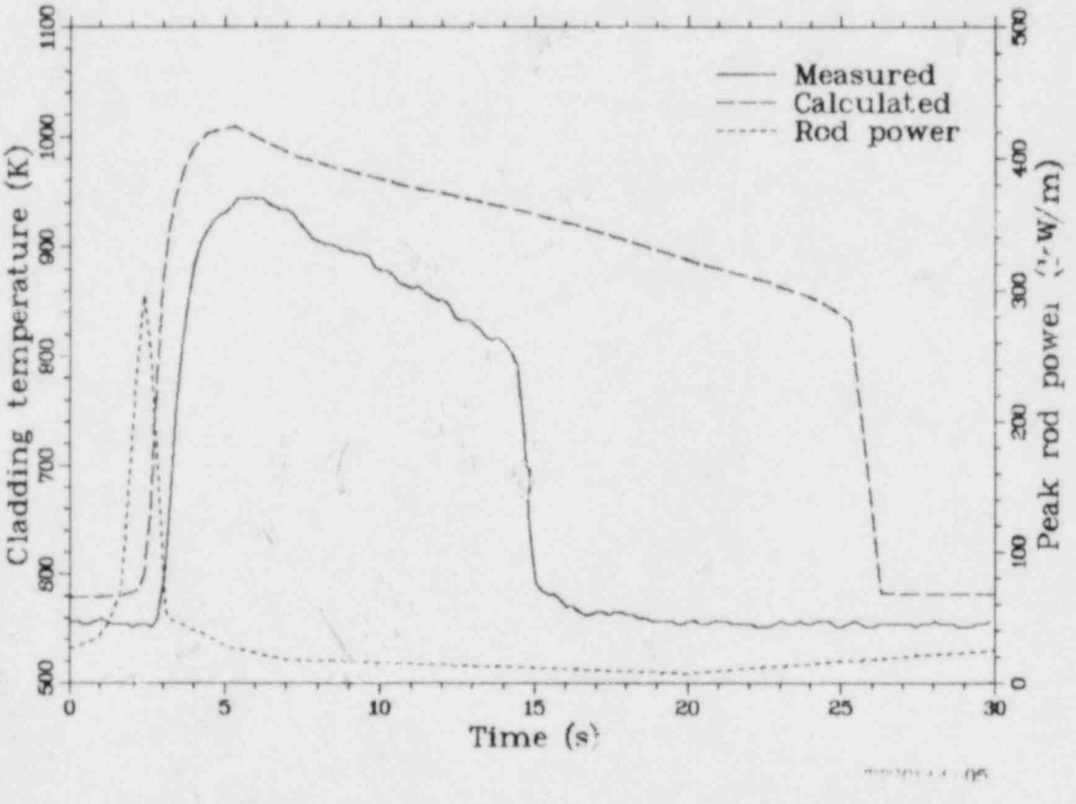

Figure 10. Measured and calculated cladding temperature at 70 mm - 0° thermocouple location and peak rod power vs. time for test Rod 902-4 during Test OPT 1-2 transient.

maximum temperature of 765 K compared to a FRAP-T6 calculated maximum of 616 K. The calculated temperature is also predicted to peak about 2 s earlier than that measured.

The thermocouple at 70 mm on Rod 902-2 (Figure 9) probably failed after reaching a temperature of 1068 K. The thermocouple indicates the cladding quenched at ~17 s, about 9 s prior to that predicted by FRAP-T6. The thermocouple at 70 mm on Rod 902-4 (Figure 10) indicated a maximum temperature of 945 K, which is only about 65 K lower and 0.5 s later in the transient than predicted by FRAP-T6. The quench time, however, is about 11 s less than predicted by FRAP-T6.

Thermocouples were intentionally not located at the axial power peak of 376 mm so that PCI cladding damage at the power peak location would not be affected. FRAP-T6 predicts a maximum cladding temperature of 1090 K at the axial flux peak, or about 80 K higher than at the 70 mm elevation.

3.3 Test Rod Cladding Strain

A comparison of the measured and calculated cladding elongation for Test Rod 902-4 and the test rod power are shown in Figure 11. The LVDT for Rod 902-2 was not operable during the transient. The maximum measured cladding elongation change during the transient (11.3 mm) was much larger than that predicted (2.2 mm). The FRAP-T6 calculations were made using the FRACAS-II model option. FRACAS-II uses a thick cladding shell deformation subcode that has a fuel cracking and relocation model applied to both the thermal and structural calculations, and a stress-induced pellet deformation model. FRACAS-II is recommended for modeling PCI power ramp testing of BWR and PWR fuel rods. Structural gap closure was predicted to occur at 2.4 s and to remain closed until about 50 s. The data shows that the gap was closed at the initiation of the transient.

Based on the 6 mm permanent measured elongation of the test rods after the transient, it is expected that the cladding collapsed onto the fuel column and into pellet interfaces at high temperature ("waisting"). Gaps between the pellets probably developed after the transient during cooldown because the cladding was locked to the pellets at each pellet interface.

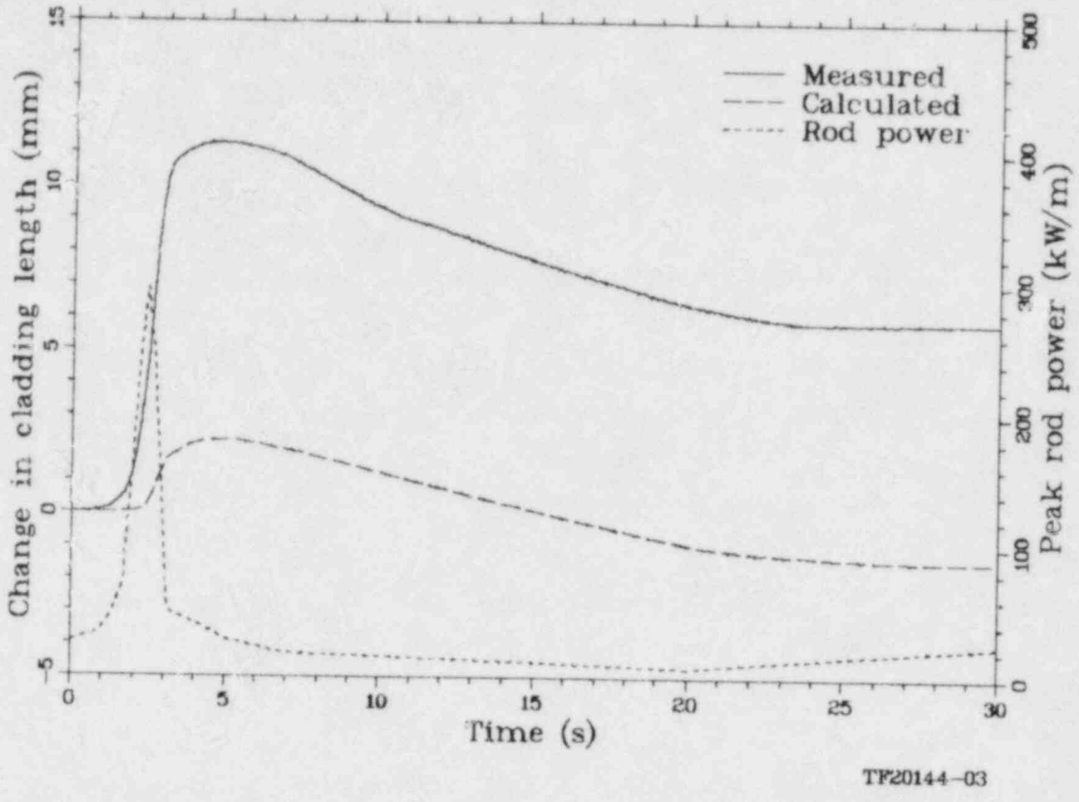

Figure 11. Measured and calculated change in cladding length and peak rod power vs. time for test Rod 902-4 during Test OPT 1-2 transient.

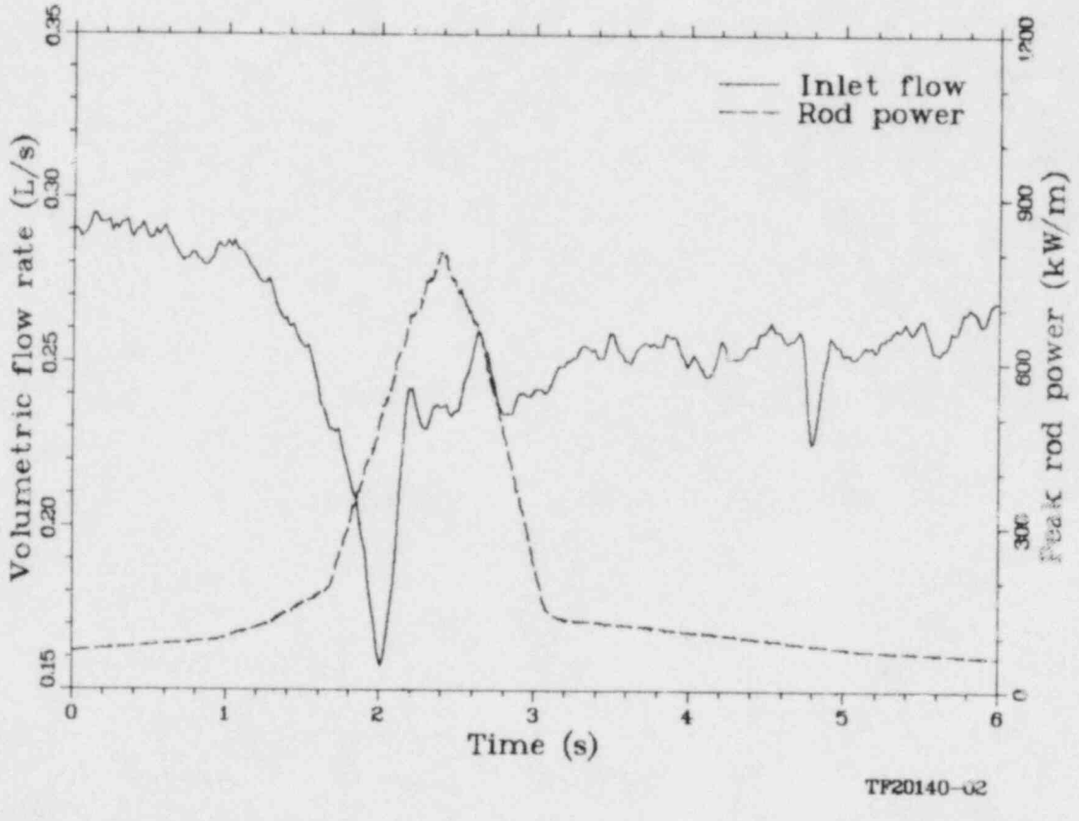

Figure 12. Inlet volumetric flow rate and peak rod power vs. time for heater Rod 902-3 during Test OPT 1-2 transient.

The maximum calculated hoop strain and hoop stress were 0.61% and 120 MPa, respectively. FRAP-T6 calculated a cladding failure probability of 2.5% due to cladding overstress.

3.4 Coolant Flow Rate

Figure 12 illustrates the inlet coolant flow and fuel rod power for Rod 902-3, one of the heater rods. Note that as the rod power increased during the power transient, the inlet coolant flow decreased briefly by about 50%. The flow decrease is caused by the prompt heating of the water from the high gamma and neutron flux during the transient and the increased heat flux from the heater rod. As shown in Figure 13, the rapid increase in the heater rod power resulted in about a 60% increase in the inlet flow for Test Rod 902-2 due to the formation of higher quality coolant and momentary expulsion of the coolant out of the heater rod flow shroud. The outlet flow meter for Rod 902-2 was inoperable during the test. The inlet and outlet flow rates for Test Rod 902-4 are shown in Figure 14. The inlet flow increased about 45%, while the outlet flow increased about 70% during the transient. The higher outlet flow increase is due to the larger steam fraction at the shroud outlet at higher powers.

3.5 Heater Rod Transient Data

The heater rods' initial power was ∿70 kW/m which increased to ∿830 kW/m at the time of peak power. The FRAP-T6 calculation predicted a radially-averaged peak fuel enthalpy of 267 cal/g UO_2. About 65% of the heater rod fuel pellet radius at the axial power peak was predicted to become molten during the transient. A maximum cladding surface temperature of 1955 K was predicted and essentially the whole cladding length was expected to reach temperatures in excess of 1150 K. The code predicted a 66.6% failure probability due to overstress (maximum hoop stress of 320 MPa).

A comparison of the measured and cladding axial elongation for Heater Rod 902-1 is shown in Figure 15. The measured elongation change is about 50% larger than that calculated (5.4 versus 3.5 mm). The momentary dip in

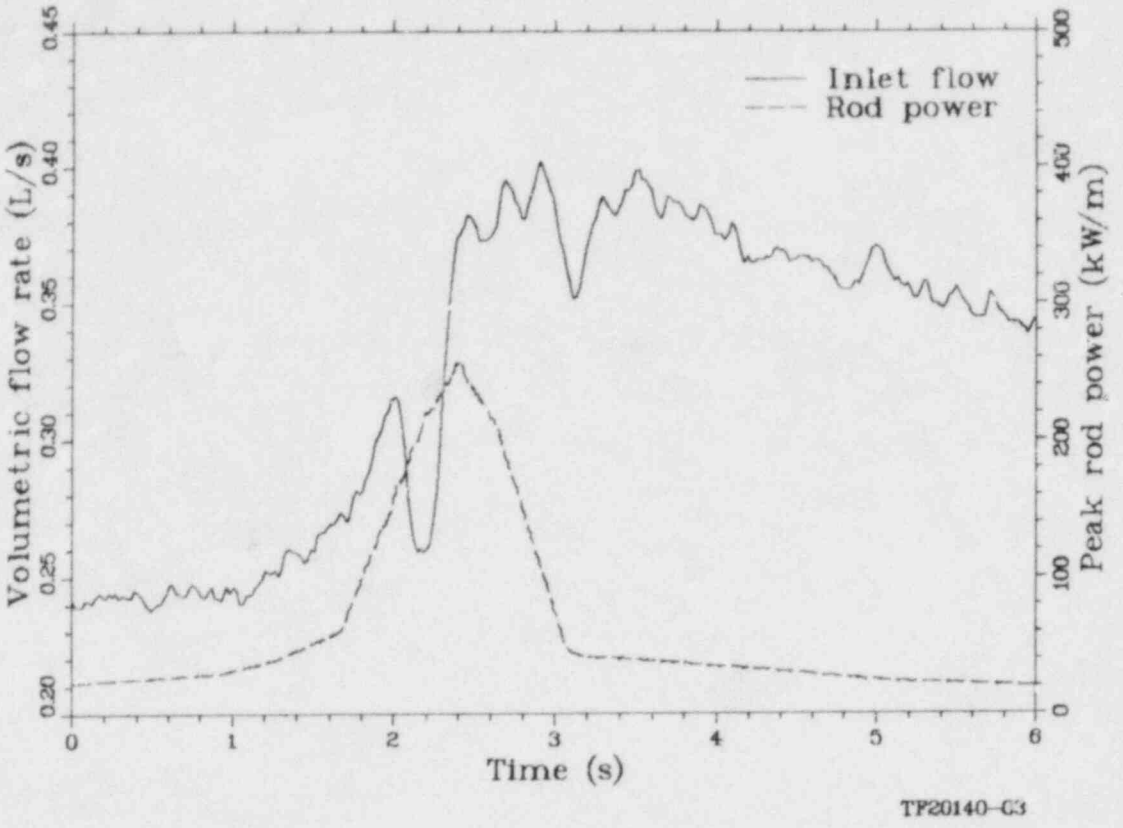

Figure 13. Inlet volumetric flow rate and peak rod power vs. time for test Rod 902-2 during Test OPT 1-2 transient.

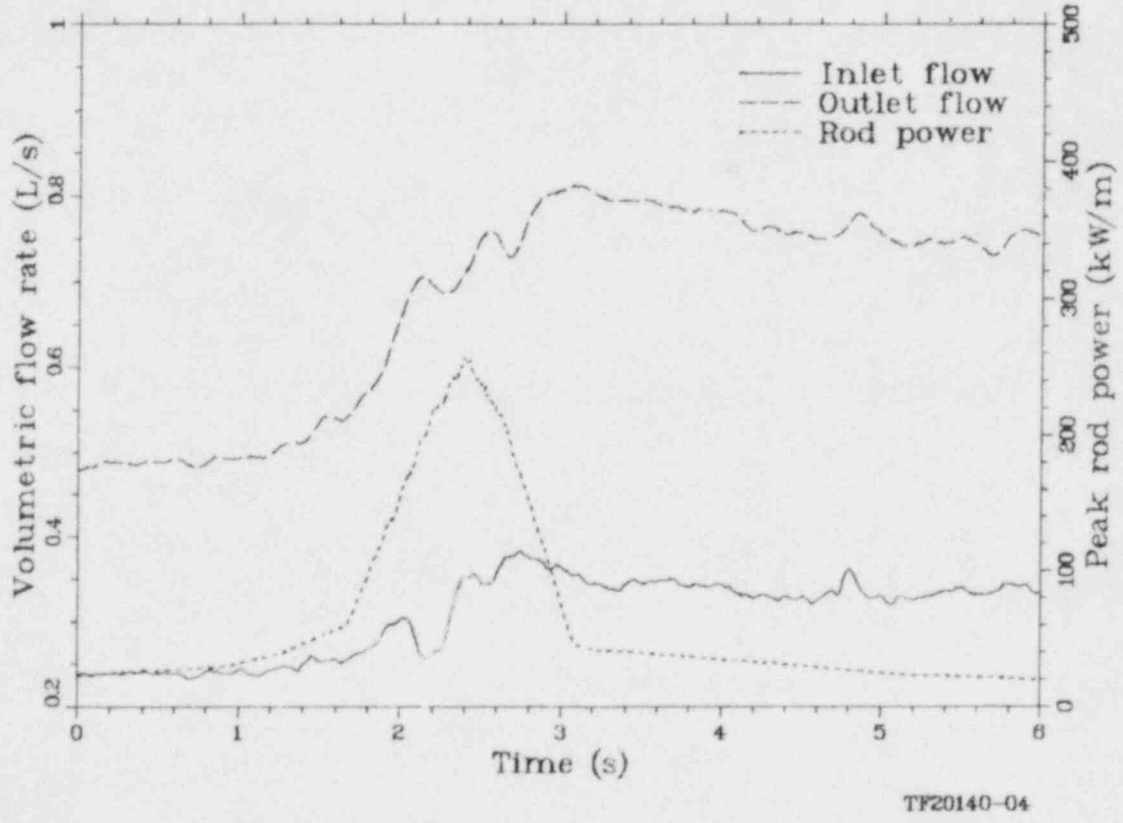

Figure 14. Inlet and outlet volumetric flow rate and peak rod power vs. time for test Rod 902-4 during Test OPT 1-2 transient.

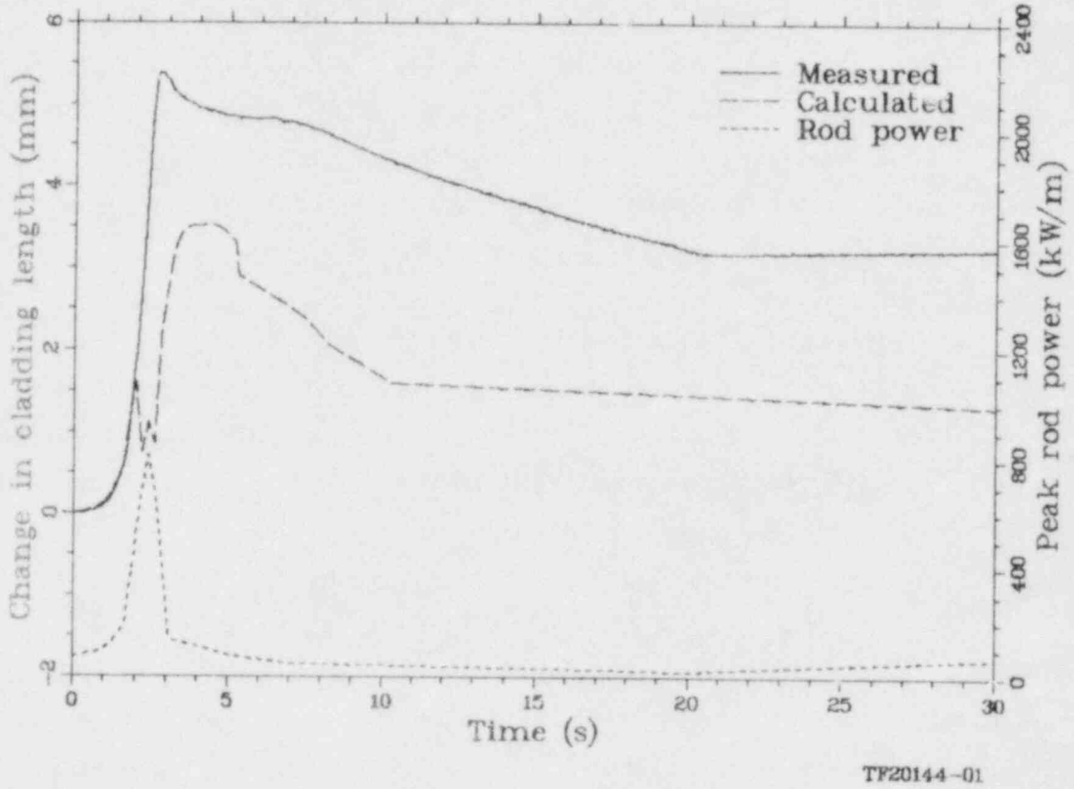

Figure 15. Measured and calculated change in cladding length and peak rod power vs. time for heater Rod 902-1 during Test OPT 1-2.

the calculation elongation at the time of peak power is caused by the zirconium phase change from alpha to alpha + beta at a temperature of 1090 K. Collapse of the heater rod cladding on the pellet stack and into pellet interfaces is expected. A ~3 mm permanent elongation change was measured. Gaps in the pellet stack probably developed after the transient during cooldown.

3.6 Fission Product Release Data

Fission product release to the PBF loop coolant was observed by the fission product detection system (FPDS) during preconditioning and following the OPT 1-2 transient. During preconditioning of the fuel rods, an indication of apparent rod failure was seen on three different instruments. As described earlier, the LVDT on Rod 902-2, the loop radiation monitor (Figure 5) and the FPDS spectrometer each displayed a simultaneous change indicative of rod failure. Figure 16 shows the measured activity of four isotopes during this time period. Approximately 15 other isotopes showed increases in coolant activity at the same time. The modest concentration levels of the isotopes are indicative of a small cladding breach, perhaps a PCI-type defect.

The fission products measured in the coolant by the FPDS were primarily the gaseous isotopes. This is in contrast to previous PBF fuel failure tests when iodine isotopes were found in abundance. The probable reason for the missing iodine is the modest fuel damage and lack of coolant exchange with the OPT 1-2 fuel rod interior. A small cladding breach may have allowed gas release but prevented coolant dissolution of iodine within the rod. In previous PBF tests where significant iodine was found in the coolant, the fuel rods were severely damaged, fuel was extensively shattered, and coolant was continuously washing through the test debris. Several of the fission products continued to rise slowly in coolant concentration throughout preconditioning.

Prior to the transient, coolant activity levels were nearly steady at a moderately high level (see Figure 17). Following the transient, the gross activity level increased approximately 20%; and following reactor

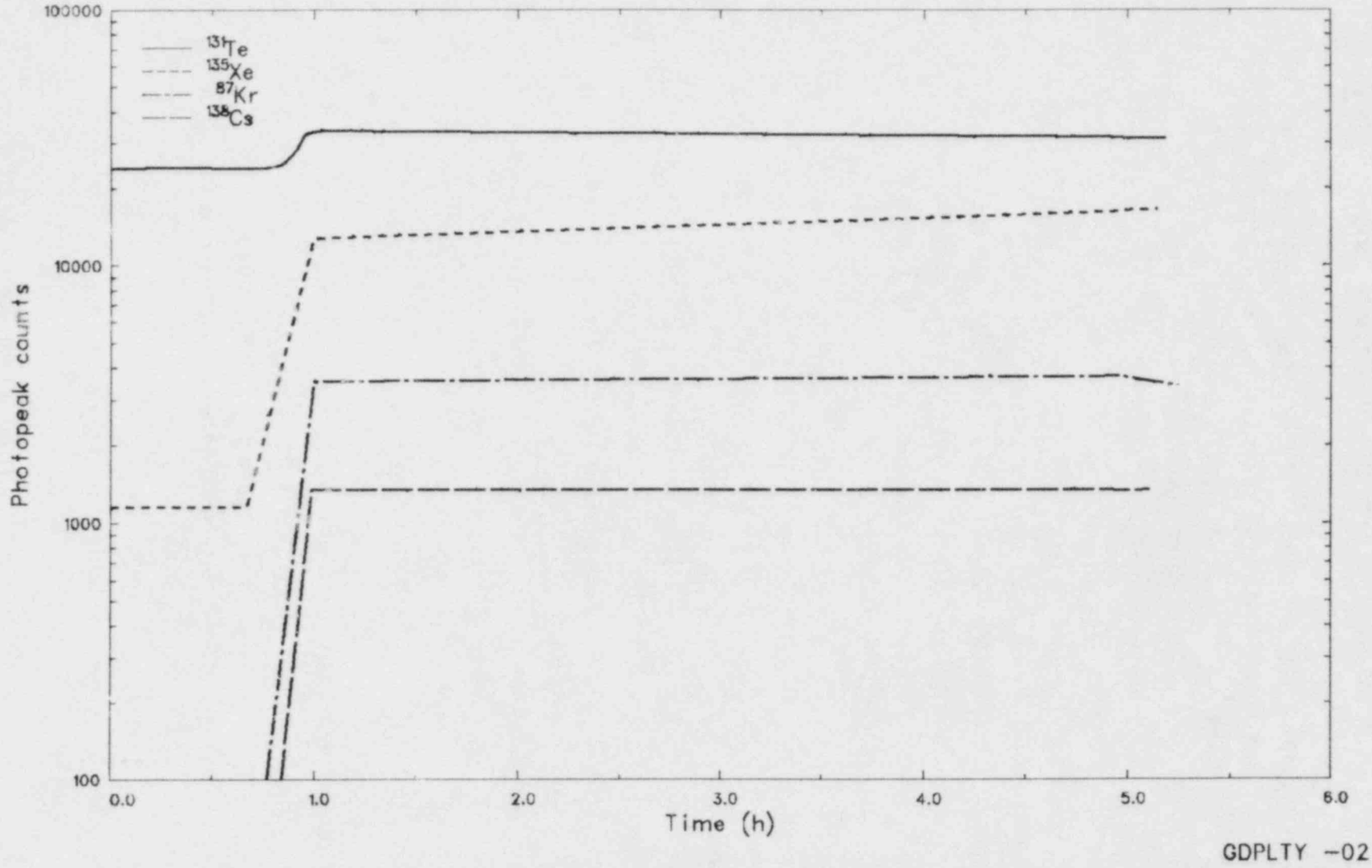

Figure 16. Coolant radioactivity levels of selected isotopes during steady-state preconditioning.

scram the activity level again increased another 10% indicating increased damage to the fuel rod, probably an enlargement of the preexisting defect.

As illustrated by the gross gamma activity shown in Figure 17, a spike release of activity appeared at the detector station ~60 s after initiation of the large power pulse in the OPT 1-2 transient. This is consistent with the 65 s delay time measured by the FPDS during the ^{153}Sm sample injection. A second but smaller spike of activity appeared at the detector station about 40 s later. The first spike is believed to be indicative of a puff release of fission products from a failed rod during the large power pulse. The second, smaller spike is believed to be a similar response to the small power pulse that was generated in OPT 1-2 between 20 to 35 s after the first pulse. The second power pulse was smaller in peak power, but longer in duration, producing a second fission product puff release nearly as large as the first.

Following the puff releases of activity, fission products continued to circulate around the PBF loop becoming more evenly distributed in the coolant. The second pass of the activity by the FPDS can be seen in Figure 16 at about 350 s. The equilibrium concentration attained 900 s after the transient was ~20% higher than the pre-transient concentration. Reactor scram occurred 1200 s after the transient, and the concentration of fission product activity increased another 10% beginning ~60 s after scram. Fission product release following scram has been seen in other PBF tests with failed fuel. The release is believed to be due to the change in fuel rod and defect geometry as power is removed, and the greater propensity for coolant exchange with the damaged rod interior.

The fission product concentrations in the loop coolant were monitored continuously by the FPDS for several hours following the transient. This information should provide a new lower bound for fuel damage with fission product release measurements, and fuel condition monitoring techniques will be enhanced by this enlarged data base.

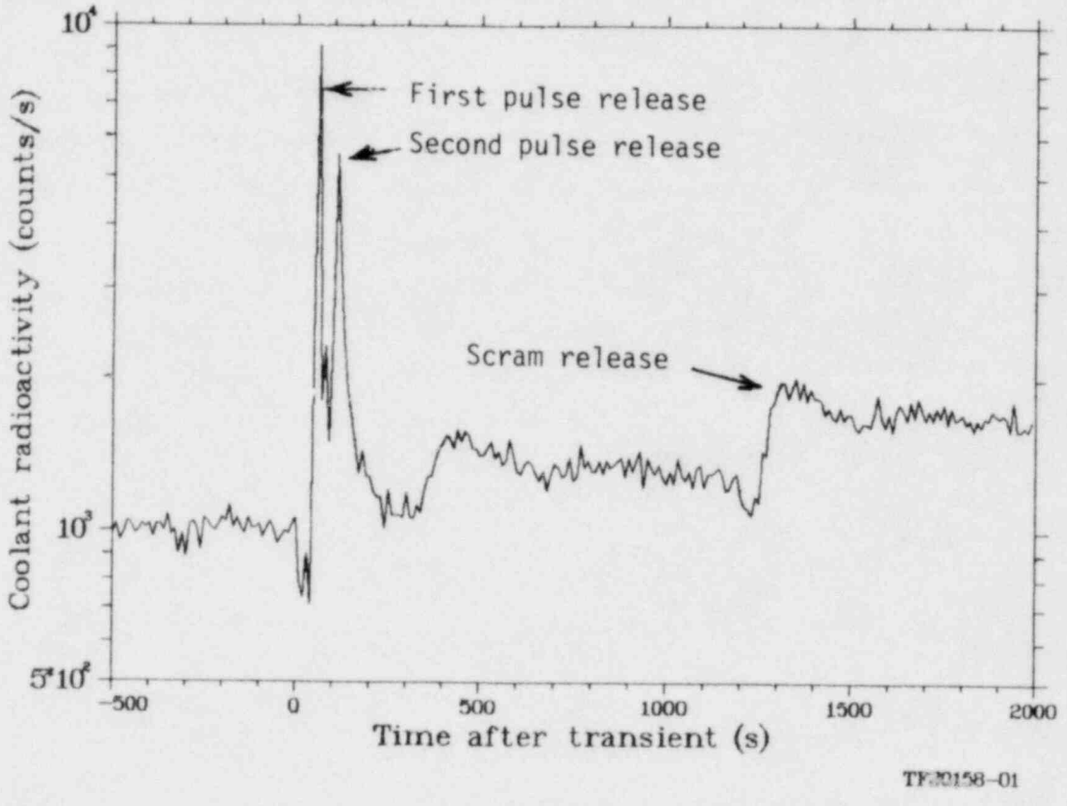

Figure 17. FPDS gross gamma detector response during the OPT 1-2 transient.

4. CONCLUSIONS

The objective of Test OPT 1-2 was to evaluate the probabilty and extent of fuel rod damage during a severe anticipated BWR transient without scram that results in boiling transition. A power transient representative of the rod power and coolant conditions calculated to occur during a BWR main steam isolation valve closure without scram was successfully performed. Maximum cladding surface temperatures of ~1070 and 950 K, which were within the temperature range sought, were measured on the two test rods. Based on the data from the cladding elongation sensors, it is expected that the cladding collapsed onto the fuel pellets and pellet interfaces over the region of the fuel rod reaching elevated temperatures. The fission product detection system indicated that one or more of the fuel rods was leaking after the transient. Since a leak had developed in either one of the two heater rods or one of the irradiated test rods during the fuel conditioning operation prior to the power transient, it is not possible to determine from the on-line data if the test fuel rods failed as a result of the transient. Metallurgical examination will be performed to identify which rod failed prior to the transient and the extent of cladding damage and determination of the damage mechanisms incurred during the transient.

5. REFERENCES

1. NRC Staff, Anticipated Transients Without SCRAM for Light Water Reactors, NUREG-0460, Vols. I and II, April 1978, Vol. III, December 1978, Vol. IV, March 1980.

2. General Electric Co., Assessment of BWR Mitigation of Anticipated Transients Without SCRAM, Volume II, NEDO-24222, February 1981.

3. M. F. Lyons et al., High Performance UO_2 Program First Pinhole Fuel Rod Failure During Center Melt Operation, Assembly EPT-12-C-A, GEAP-5100 K, 1966.

4. Preceedings of the KTG/ENS/JRC Meeting on Ramping and Load Following Behavior of Reactor Fuel, November 30 to December 1, 1978.

5. W. J. Bailey et al., State-of-the-Technology Review of Fuel Cladding Interaction, COO-4066-2, PNL-2488, December 1977.

6. J. T. A. Roberts et al., "On the Pellet-Clauding Interaction Phenomenon," Nuclear Technology 35, August 1977, pp. 131-144.

7. E. E. Lewis, Nuclear Power-Reactor Safety, Wiley and Sons, 1977.

8. J. H. Davies et al., Irradiation Tests to Characterize the PCI Failure Mechanism, NEDO-21551, February 1977.

9. C. L. Mohr, PCI Fuel Failure Analysis: A Report on a Cooperative Program Undertaken by Pacific Northwest Laboratory and Chalk River Nuclear Laboratory, NUREG/CR-1163 PNL-2755, December 1979.

10. R. K. McCardell, Z. R. Martinson and P. E. MacDonald "Damage and Failure of Previously Irradiated Fuel Rods During a Reactivity Initiated Accident", Proceedings of ANS Topical Meeting on Thermal Reactor Safety, Sun Valley, Idaho (August 1981).

11. D. W. Croucher, M. K. Charyulu, Experiment Requirements for the Study of Anticipated Transients With and Without Scram, TFBP-TR-308, January 1979.

12. D. T. Sparks, OPTRAN 1-2 Experimental Specification Document, TFBP-TR-317, Revision 2, January 1981.

13. W. P. Polkinghorn, OPT 1-2 Experiment Configuration Specification, ES-50640, November 1981.

14. Z. R. Martinson and R. H. Smith, Operational Transient Test Series, Test OPT 1-2, Experiment Predictions, EGG-TFBP-5601, November 1981.

15. Z. R. Martinson, Operational Transient Test Series, Test OPT 1-2, Experiment Operating Specification, EGG-TFBP-5600, Revision 1, May 1982. Including the following document revision: Document Revision Request--No. 364, May 1982.

16. L. J. Siefken et al., FRAP-T6: A Computer Code for the Transient Analysis of Oxide Fuel Rods, NUREG/CR-2148, EGG-2104, May 1981.

17. G. A. Berna et al., FRAPCON-2: A Computer Code for the Calculation of Steady State Thermal-Mechanical Behavior of Oxide Fuel Rods, NUREG/CR-1845, December 1980.

APPENDIX A
EXPERIMENT DESIGN FOR TEST OPT 1-2

APPENDIX A
EXPERIMENT DESIGN FOR TEST OPT 1-2

A summary description of the fuel rod, test train, and instrumentation for Test OPT 1-2 is provided in this section.

A-1 Fuel Rods and Shrouds

Two preirradiated BWR 8 x 8 segmented test rods, provided by the General Electric Co., and two unirradiated 10% enriched fuel rods used to heat the coolant for the test rods were tested. The two unirradiated heater rods were designated 902-1 and 902-3 and the two preirradiated test rods were designated 902-2 and 902-4. The fuel rod designation and burnups are given in Table A-1. The nominal design characteristics for the OPT 1-2 fuel rods are given in Table A-2.

Each test fuel rod was surrounded by a coolant flow shroud. The shrouds were fabricated from zircaloy-4 tubing with a circular cross section with an inner diameter of 19.05 mm and an outer diameter of 22.05 mm. The outlets of the flow shrouds for Rods 902-1 and 902-3 are connected by 14.3 mm inner diameter tubing to the shroud inlets of Rods 902-2 and 902-4, respectively.

Remotely operated orifices, installed at the shroud outlets for Rods 902-1 and 902-3, provided a bypass for the coolant exiting the heater rods. The test rod inlet flow was reduced by ~55% when the orifices were fully opened.

A-2 Test Train

A Battelle Northwest Laboratory four rod test train was modified and used for OPT 1-2. The test train positions and supports the four fuel rods in the inpile tube (IPT). The IPT flow tube directed the coolant from the IPT inlet down to the lower plenum and up into the heater rod flow shrouds. Each fuel rod was fixed rigidly to the shroud at the top of the fuel rod and was free to expand axially downward against a linear variable

TABLE A-1. TEST OPT 1-2 FUEL ROD DESIGNATIONS AND BURNUPS

PBF OPTRAN Designation	Original Rod Designation	Rod Type	Burnup (GWd/t)	Original Core Axial Location[a]
902-1	N. A.	Reference	0	N. A.
902-2	OD07-4	Reference	9.6	Top
902-3	N. A.	Reference	0	N. A.
902-4	OA06-4	Reference	8.0	Top

a. Segmented test rods were irradiated in a bundle located on the extreme periphery of the Monticello Boiling Water Reactor owned and operated by Northern States Power Company. Four segmented rods were threaded together to form a ~3.86 m long rod.

TABLE A-2. TEST PT 1-2 FUEL ROD DESIGN CHARACTERISTICS

Characteristics[a]	GE 8 x 8 Rods	Heater Rods
Fuel		
Material	UO_2	UO_2
Enriched pellet stack length (mm)	752.6[b]	752.6
Pellet outside diameter (mm)	10.57/10.62[c]	10.57
Pellet length (mm)	10.66	10.66
End configuration	chamfer	chamfer
Density (%TD)[d]	95 to 96	95 to 96
Initial enrichment (wt%)	2.87	10
Cladding		
Material	Zr-2	Zr-2
Tube outside diameter (mm)	12.52	12.52
Tube inside diameter (mm)	10.80	10.80
Cladding thickness (mm)	0.86	0.86
Fuel Rod		
Overall length (mm)	1133.35	953.5
Gas plenum length (mm)	139.7	50.8
Flux depressor pellets	92.3% HfO_2-7.7% Y_2O_3	none
Diametral gas gap (mm)	0.229/0.178[c]	0.229
Fill gas composition	As received	Helium
Fill gas pressure	As received	0.31 MPa
Getter assembly outside diameter (mm)	6.10	none
Getter assembly length (mm)	50.8	none
Shrouds		
Material	Zr-4	Zr-4
Tube outside diameter (mm)	22.225	22.225
Tube inside diameter (mm)	19.05	19.05
Connecting line outside diameter (mm)	15.88	17.48
Connecting line inside diameter (mm)	13.89	14.29

a. Data are preirradiation values.

b. Pellet stack also contains 12.7 mm of hafnium-yttrium oxide pellets at each end of fuel column. Total length 778 mm.

c. 0007-4/0A06-4

d. Theoretical density (TD) of UO_2 is 10.97 g/cm^3.

differential transformer (LVDT), that measured the axial growth of each rod. The 0.75 m long fuel rods and shrouds were positioned such that the axial midplane of the active fuel stack was at the same elevation as the axial midplane of the PBF core fuel rods which are 0.91 m long. The fuel rods were centered in the shroud with two sets of centering screws located at ±254 mm from the fuel midplane. A spring mechanism was installed on one of the two centering screws at each axial elevation.

A-3 Instrumentation

A brief description of the OPT 1-2 instrumentation is provided in this section. Since none of the fuel rods were opened in order to maintain the fuel chemistry in the irradiated rods, no rod internal instrumentation was used. The fuel rod and test train instrumentation consisted of the following:

1. The two irradiated rods (Rods 902-2 and 902-4) were each instrumented with three thermocouples (6 thermocouples made of 0.70 mm diameter, zircaloy sheathed tungsten-rhenium) resistance welded to the cladding outer surface. One thermocouple on each of Rods 902-2 and 902-4 was located at the 0° orientation (towards the test train axial centerline) and 70 mm above the axial midplane of the test rod fuel. A second thermocouple[a] on each rod was located at 120° and +170 mm, and the third at 240° and +270 mm.

2. A 0.51% cobalt--99.49% aluminum flux wire each enclosed in a small diameter zircaloy tube, located on the outer wall of each flow shroud, to measure neutron fluence.

3. A LVDT, located at the location of each rod, to measure cladding elongation.

---

a. The thermocouple located at 170 mm-120° on Rod 902-2 was not successfully resistance welded to the cladding. The thermocouple was attached by using a small zircaloy strap which was resistance welded to the cladding on each side of the thermocouple tip.

4. A 69 MPa pressure transducer located near the upper particle screen to measure coolant pressure pulses.

5. A 13.8 MPa pressure transducer located outside the IPT head connected by tubing to the midplane of flow shroud 902-2 to measure normal system pressure.

6. A 13.8 MPa pressure transducer located outside the IPT head connected by tubing to the midplane of flow shroud 902-4 to measure normal system pressure.

7. A 13.8 MPa pressure transducer located outside the IPT head connected by tubing to sense the pressure just above the shroud outlet of Rod 902-4.

8. A turbine flow meter located at the inlet of each flow shroud of Rods 902-1 and 902-3 to measure experiment coolant flow.

9. A turbine flow meter located in the cross-over tube of Rods 902-2 and 902-4 to measure inlet flow.

10. A turbine flow meter located at the outlet of flow shrouds 902-2 and 902-4 to measure coolant flow. The flowmeter on shroud 902-2 was inoperable during the test.

11. A Chromel-Alumel (type K) thermocouple mounted at the inlets of each flow shroud to measure inlet coolant temperature.

12. A Chromel-Alumel (type K) thermocouple mounted near the outlets of each flow shroud to measure outlet coolant temperature.

13. A Chromel-Alumel (type K) thermocouple mounted above the variable orifice outlet of Rods 902-1 and 902-3 to measure outlet coolant temperature.

14. A platinum resistance thermometer (RTD), located in the inlet region of the test train, to measure coolant inlet temperature.

15. Four pairs of Chromel-Alumel (type K) thermocouples connected differentially, one junction located at the inlet and one junction at the outlet of each flow shroud, to measure temperature rise in the coolant.

16. Two pairs of copper-constantan (type T) thermocouples connected differentially one junction located at the inlet of the flow shroud and one junction at the outlet of the variable orifice of flow shrouds 902-1 and 902-3, to measure temperature rise in the coolant.

17. Twelve self powered neutron detectors (SPNDs), one each in quadrants 2 and 4, and 2 strings of 5 SPNDs located in quandrants 1 and 3.

18. Two U-235 fission chambers and two detectors for gamma compensation located in quadrant 2 and 4 to measure relative neutron flux.

19. Two platinum self-powered gamma detectors (SPGD) located in quadrant 1 and 3 to measure relative gamma flux.

20. Variable orifice position (2).

21. Variable orifice line pressure (2).